





Research Article

Two Stop-Line Method for Modern T-Shape Roundabout: Evaluation of Capacity and Optimal Signal Cycle

Khurrum Jalil ¹, Yuanqing Xia ¹, Muhammad Noaman Zahid ²,
and Md Abdus Samad Kamal ³

¹School of Automation, Beijing Institute of Technology, Beijing 100081, China

²School of Information, Hunan University of Humanities, Science and Technology, Loudi 417000, China

³Graduate School of Science and Technology, Gunma University, Kiryu 376-8515, Japan

Correspondence should be addressed to Yuanqing Xia; xia_yuanqing@bit.edu.cn

Received 5 January 2022; Revised 14 March 2022; Accepted 12 April 2022; Published 4 May 2022

Academic Editor: Jing Zhao

Copyright © 2022 Khurrum Jalil et al. This is an open access article distributed under the Creative Commons Attribution License, which permits unrestricted use, distribution, and reproduction in any medium, provided the original work is properly cited.

Uncoordinated traffic flows at the traditional roundabouts, especially with a small circumference and fewer lanes, are often heavily affected by congestion, which escalates fuel consumption, CO₂ emissions, idling, and travel delay. An intriguing way to mitigate such uncoordinated flows at junctions would be facilitated through optimal traffic signalization. For this purpose, this paper presents a novel holistic Three-Leg Signalized Roundabout (TLSR) model based on two signalized stop lines (2SL). The first stop line is placed at each entry curve of a roundabout with effectual lane markings as usual. Hereafter, the second stop line is set exclusively in the circulatory roadway to improve left-turning mobility with an additional “short-lane model” to deal with heavy traffic, following specific patterns for smooth vehicle merging. The capacity and optimal signal cycle relationships are derived to evaluate the performance of the proposed TLRS-2SL, considering the internal space constraints of the roundabout. Under the various scenarios, the parameters’ sensitivity tests demonstrate that signal cycle and central radius play a significant role in enhancing the roundabout’s operational performance. From the executed simulation, the proposed framework improves the traffic flow by 15% and controls the relative error within 10% compared to benchmark methods.

1. Introduction

Due to the tremendous vehicle influx, the existing road infrastructure seems less capable of managing traffic in peak hours. Scholars have presented two feasible solutions to alleviate the congestion sharply. The first solution includes extra construction of flyovers or underpasses, enlarging the number of lanes near intersections, expanding major roads’ dimensions, and the conversion of stop-control junctions into intersections or roundabouts. Nevertheless, such expansions of the existing infrastructures disturb the traffic flow network, need extra efforts, and cause financial burdens. The second solution is to use innovative markings at existing structures and to design reasonable signal cycles for the roundabouts, intersections, and stop control junction, or where further construction is not possible [1–4].

The U.S. Department of Transportation (DOT) defines a roundabout as “a circular configuration of roadways with

yield control featuring on all entering arms, one-way continuous flow within the circulatory lanes along with channelization of approaches, and appropriate geometric curvature to keep flow circulating speed low” [5]. Besides that, the circulatory flow has priority to move, while approaching vehicles are obliged to give them a pathway according to “priority to the circle rule” [6]. One of the possible reasons of vehicle braking is when approaching vehicles decelerate to enter the roundabout, and the merging points of the section are already engaged due to the circulatory flow. In this scenario, vehicle disorder will occur if there is no traffic control system.

In addition, the roundabout without a control system has been investigated extensively (e.g., mainly focused on geometric designs) [7]. On the other hand, signalized roundabouts are studied more than nonsignalized ones, and the proposed control plans and designs are successfully implemented in the real world to eliminate possible conflicts

[2, 8]. The survey showed that casual and fatal accidents are significantly reduced by using signal entries at roundabouts [9]. In addition, the study shows that if the single- and double-lane signalized intersections are converted to a modern roundabout, then the injury crashed modification factor would be decreased up to 60% [10]. In Scotland, the traffic signals installation at the roundabout was proven to be effective [11]. The case study in Sheffield, UK, discovered that signal installation is the best and most economical solution for balancing the entry flows between each approach [12].

Wong et al. [13] conducted a research survey of four different spiral-marking roundabouts in Hong Kong. The survey output discovers that drivers support these unique lane-marking projects, perceiving these projects is safer, accidents are reduced, conflicts are decreased, cost-efficient, and easy to execute in the real world. Generally, the lane markings exist beside the entry curve of roundabout usually called concentric lane-marking or Alberta markings, and the spiral lane markings are those round- (circular-) shape markings, which is drawn for separating the vehicles in the circulatory roadway, as shown in Figure 1(a) [14]. Xue et al. [15] presented the optimization process to control the traffic at the roundabout using a fixed signal cycle.

Furthermore, Bie et al. [8] have proposed Stop-Line Setback (SLSB) method and suggested that signalized stop line placed 15–20 m backside from the entry curve of the roundabout with proper markings, especially for that single arm of the roundabout, where the flow is supposed to be heavy. The proposed SLSB method uses the adaptive level signal control scheme for the convenient crossing of flow. Furthermore, traffic engineers utilized different metering techniques to supervise an inequitable roundabout flow [16, 17]. Although these techniques provide promising results to improve mobility, the conflicts with opponent vehicles in circulatory lanes cannot be eliminated by using these studies. Ma et al. [18] developed an integrated optimization model that can evaluate the lane markings and timings of a signalized roundabout, especially to control the vehicle's turning movements. Furthermore, traffic practitioners have spent their outstanding efforts to present different solutions to improve the mobility at the roundabout (e.g., signal timing process [19], fixed signal cycle [15], futuristic approaches [20], capacity [21, 22], delay [23, 24], safety [25], and for intersections [26]).

Moreover, Yang et al. [2] discovered the two-stop-line method to enhance the roundabout capacity in which the second signalized stop line is exclusively set in the circulatory roadway to improve the efficiency of left-turning flow at the four-legged roundabout. The project is successfully implemented in Xiamen, China. Jiang et al. [1] proposed a two-stop-line signalized roundabout (TSLSR) model to control the left-turning flow, considering various roundabouts radii and optimal signal cycles for evaluation. Sun et al. [27] presented a comparative analysis between the signalized intersection and the signalized and nonsignalized roundabout to measure the left-turning traffic capacity, using the two-stop-line method. However, most of the two-stop-line techniques were developed for X-shape

roundabout, exploiting the Webster equation method for an optimal signal cycle. From the operational aspects, signalized roundabouts performed better than usual signalized intersections, and such engineering-oriented frameworks have proved low transformation cost, as well as being easy to construct and implement.

In the aforementioned literature, the main intention is to properly utilize the spatial and temporal constraints with optimal/advanced signalization methods to halt recurring congestion at the roundabout. Usually, roundabouts tend to exhibit severe operational problems due to an unbalanced pattern of left-turning directional flow. The Washington DOT presented brief guidelines for a T-shape roundabout with different methodologies and structural design by summarizing multiple kinds of literature [5]. As shown in Figure 1(b), the flow of the T-shape roundabout is generally divided into two phases where Phase 1 (P_1) organizes the traffic of east and west approaches and Phase 2 (P_2) is set for the south section. During the green time of P_1 , the east left-turning flow has a conflict with the west straight-going flow. Conventionally, the problem can be addressed by setting an exclusive second stop line along with reasonable signal-timing in the circulatory. However, there are few studies proposed, especially for the T-shape roundabout to address such conflict and congestion problems using the two-stop-line method.

In the proposed study, a new signal control method is proposed for a T-shape roundabout to resolve the traffic congestion, eliminating the conflicts at merging points (e.g., points, A, B, C, D), as shown in Figure 1(d). The first stop line is placed at each entry curve of the roundabout with effectual lane markings as usual, and the second stop line is set exclusively in the circulatory roadway, following the specific patterns for smooth vehicle merging. A short-lane model is also developed for specific left-turning traffic to resolve the complex traffic phenomena in rush hours. Traffic signals are installed at each stop line with the proper phase sequence according to roundabout specific design to improve the promising mobility and safety. The capacity and optimal signal cycle equations are derived to evaluate the operational performance of the proposed TSLSR-2SL, considering the internal space constraints of the roundabout with a limited queue length. Apparently, the immediate attention of modern TSLSR-2SL is to manage the heavy flow, balance the states of all approaching vehicles, achieve proper use of spatial constraints, regulate circulatory flow without any deadlock conditions, debottleneck, improve travel time, increase capacity, and reduce the number of idling conditions at merging point. Hence, the precision of model parameters is considered very sensitive to maximize the capacity.

The executed simulations are examined under [60 s~160 s] signal cycle with inscribed circle radius [10 m~60 m] of the roundabout. Nevertheless, the results show that hypothetical TSLSR-2SL with its recoating styles has a superior performance in terms of improved capacity than the usual T-shape signalized roundabout by controlling the relative within 10% and improving the accuracy level up to 15%. To investigate deeply, the 5% proportion or influence

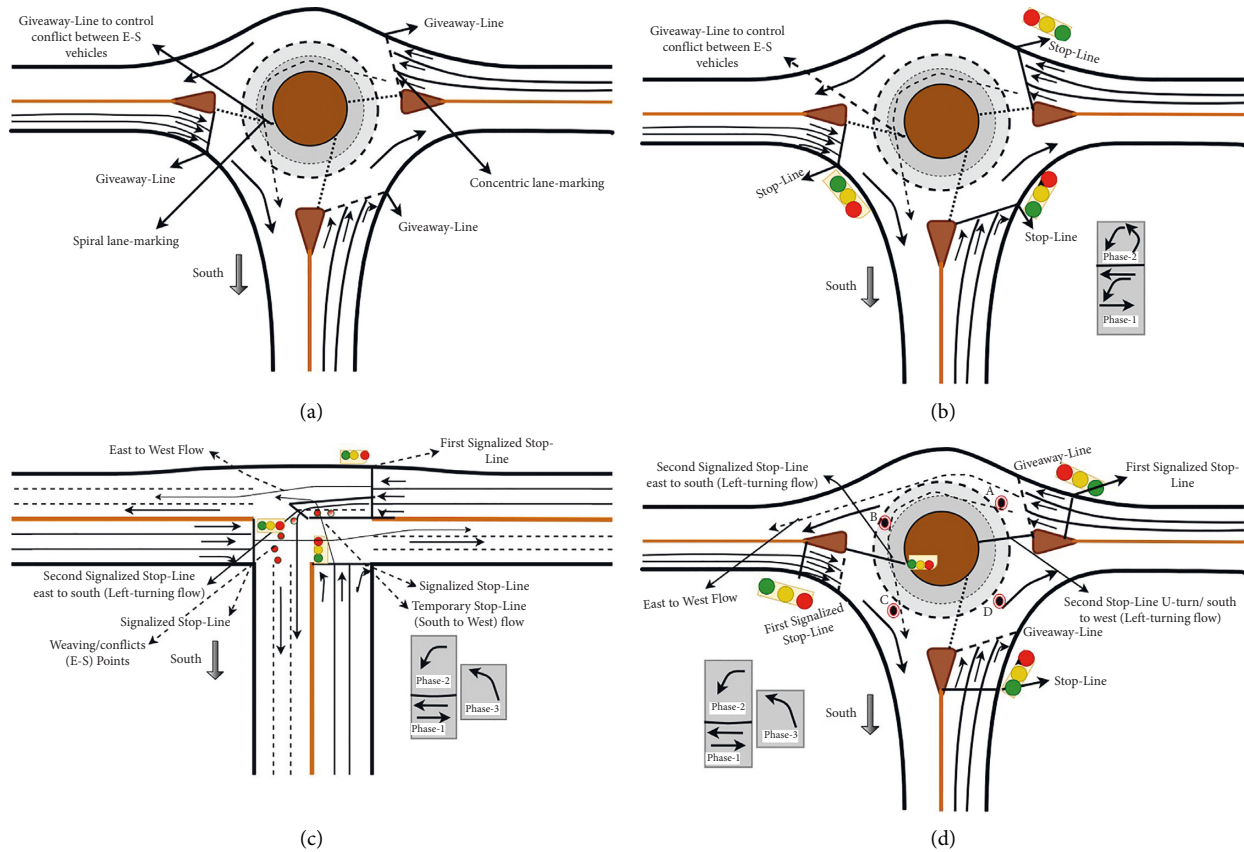


FIGURE 1: Geometry structure of roundabouts. (a) Modern roundabout. (b) Signalized roundabout. (c) Signalized intersection. (d) TLSR-2SL.

of heavy vehicle (e.g., local buses or trucks with passenger cars) is also included to make a more realistic scenario, as appearing in the real world. To the best of the author’s knowledge, no analytical work and little empirical work have yet been explored on the proposed topic.

The remaining structure of this article is organized as follows. A brief theoretical demonstration of the proposed framework is discussed in Section 2. The formulation of optimal signal cycle length, short-lane model, and capacities are computed in Section 3. Comparative numerical and sensitive analyses between models are presented in Section 4 to reveal the impact of the roundabout radius with signal cycle lengths. Finally, Section 5 presents brief discussions on simulated results, and concluding remarks with future research directions are drawn in Section 6.

2. Theoretical Evaluation of TLSR-2SL

The TLSR-2SL model is developed considering both spatial (space) and temporal (signal cycles) constraints benefits with unique lane markings. Firstly, the entry curvature of the roundabout has two obstacle lines where the first stop line is the signalized stop line, and the second line is simply the giveaway line. These lines are set beside the entry curve of the roundabout, and the distance between both lines is called the waiting area. Apparently, the traffic signal controller will not further control waiting area vehicles, and the vehicles in the

waiting area can enter circulatory lanes if there is no other flow existing. Next, to scrutinize the internal space constraints of the rotary, the second signalized stop line is placed in circulatory lanes along with a short-lane model, specially equipped to control the heavy left-turning flow. However, the method also resolves five influencing factors, namely, circulatory blockage, demand starvation, lane changing, number of potential conflicts with opposing vehicles, and multilane interference, as presented in Figure 1(d), and the real-world application Figure 2. In addition, the applicability and implementation guidelines of this new concept are presented accordingly.

2.1. Execution Plan. It is already known that nonsignalized roundabouts have just one giveaway line at the entry curvature, and the approaching flow provides a way to circulatory vehicles, as shown in Figure 1(a) [5]. Also, it has been observed that vehicles’ entry volume at individual sections can differ from the other sections and may be extremely unstable. Let the east and west sections’ entry volume be higher than the south section. In this scenario, the east-to-south (E-S) flow is greatly affected by west straight-go flow or vice versa. Consequently, the unbalanced E-S flow from the east approach is supposed to have a new strategy for efficient mobility and intercept any incidence near to point DD' or CC' , as shown in Figure 3. Hence, to counter inner



FIGURE 2: TLSR-2SL real-world application.

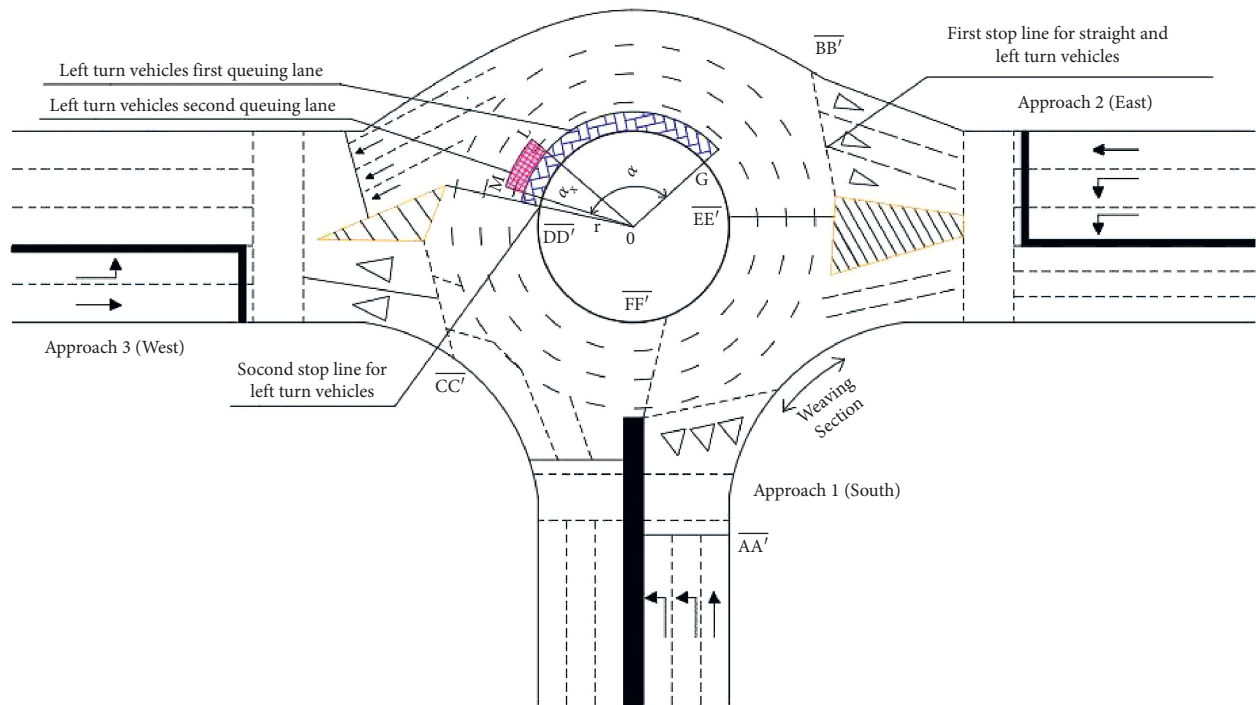


FIGURE 3: Internal space constraint of primary and secondary roadways.

circulatory conflicts, a second signaled stop line is placed to improve the rotary's operational performance with proper queue markings.

Meanwhile, P_3 is set to organize the flow from the south approach, and P_1 has to control east and west straight-go traffic streams, and P_2 is for E-S left-turning flow, as shown in Figure 1(d). As depicted in Figure 3, if the queue length of left-turning flow reaches its maximum limits in the primary lane, then the secondary trapezoid queue area is also added to treat more left-turning flow. The mathematical description of this short-lane model is given as follows in the section. Conversely, the straight-going flow from the east to the west or vice versa should find enough gaps to complete maneuvers. When P_1 is near to terminate and Phase 1 left-turning (P_2)

signal is near to execute, the vehicles that stop at the second stop-line start toward their destination.

Note that, during the termination of green time at the first signaled stop line, the vehicles at the tail of a queue may pass the signaled stop line and stay in the waiting area to avoid conflicts with opposing vehicles. The distance between the giveaway line and signaled stop line is called the waiting area, and the signal controller will not further control waiting area vehicles to ensure efficiency, as depicted in Figure 1(d). Generally, the gap between both lines is used for the convenient pedestrian crossing or nonmotor vehicles during the red phase time. Apparently, these methods are used for roundabouts with no crossing bridge or medium-sized roundabouts. The other purpose of the giveaway line is

that vehicles should enter the circulatory roadway after crossing the signalized stop line by following the safety criteria before merging. The classified flow of the waiting area towards circulatory lanes can be indicated by using the random seed probability ($p(u)$), as presented in the following equation:

$$p(u) = \begin{cases} P, & \text{if } (G_{\text{Line}} - \delta_n) \leq (G_{\text{Line}} + \delta_d), \\ P, & \text{if } \delta_d \geq 1, \\ 0, & \text{otherwise,} \end{cases} \quad (1)$$

where G_{Line} represents the giveaway line beside the entry curvature of circulatory lanes and P represents the probability. In addition, δ_n shows that there is not sufficient gap to enter inside the circulatory, and δ_d depicts the possibility to enter inside the circulatory roadway from the waiting area with the heed of safety constraints.

2.2. Principle of Traffic Signal. The rudimentary objective of signals is to assist sufficient left-turning flow through the proposed optimal signal cycles length. The position of signals is manifested with proper lane markings, as presented in Figure 1(d).

In addition, the switching between phases is based on green light termination, and a summary is defined as given below.

- (i) The switching of phase depends on its effective green time termination; for example, the green time of P_3 shifts to $P_1 \sim P_2$, after the termination of adequate green time of P_3 and vice versa, as shown in Figure 4.
- (ii) Straight-go and left-turning vehicles from the east and west approaches start to travel on P_1 , which were stopped on the first stop line.
- (iii) During P_1 , left-turn flow approaching from the east section should stop on the second stop-line at circulatory roadway instead of passing the roundabout directly, and straight-go flow continues to move without stopping again and vice versa for the west section. Further, the description of the short-lane model in the circulatory roadway is also elaborated in Section 2.3.
- (iv) After termination of P_1 , P_2 left-turning phase gets green time for vehicles having left turn, or already stop inside the circulatory roadway at any determined lane-marking point.
- (v) The roundabout has three approaches, and there is no opposite direction of the southbound. So, during P_3 , vehicles can move towards the west and take a U-turn.
- (vi) If there is a less or heavy flow, the proposed optimal signal cycle length can adjust the green duration of $P_1 \sim P_2$ or P_3 .



FIGURE 4: Phase sequence diagram.

2.3. Description of Short-Lane Model in the Circulatory Roadway. In Figure 3, point DD' is considered as second stop line and, an angle between OG and OD shows a particular queue area for E-S flow. To resolve the further disorder issue, an auxiliary short lane is added with the second stop line, and the outer part of angle LOM is supposed the short lane. Figure 1(d) shows that the saturation flow distance of E-S vehicles in the circulatory is supposed as AB and BC , where AB is considered the east-to-west flow and BC is the distance of left-turning flow. The curved circulatory lanes are denoted by α with circulatory radius angle of 90° . Suppose that x is the approach; then $\alpha_x = \alpha$ when $x = 1$, as illustrated in Figure 3. Note that the approach x of the roundabout presents one approach (e.g., east approach, and radius = circumference / (2 * π)). From the approach x , q_x should be equation (2). where r is the radius of the roundabout and w shows the weaving width, as given in the brief description of notations in Table 1. Afterward, to measure the "possible number of vehicle's queues on approach x " (C_x^l) at first signalized stop-line can be calculated by

$$C_x^l = \frac{q_x}{l_{\text{avg}}} \quad (3)$$

$$q_x = \frac{\pi \alpha_x}{180(r + 0.5w)} \quad (2)$$

Let there be n left turning lanes in circulatory roadways to assist the left-turning flow of approach x (e.g., the available circulatory lanes of traffic); moving from E-S (C_n^x) is given as

$$C_n^x = nC_x^l \quad (4)$$

The overall limited number of vehicle's queues before the second stop-line during one signal cycle (C_c^l) can be calculated by equation (5) because every approach x has limited green time in one signal cycle:

$$C_c^l = \sum_x C_n^x \quad (5)$$

Moreover, the weaving width (W_w) of lanes can be computed by

$$W_w = \left(\frac{e_1 + e_2}{2} \right) + 3.5m. \quad (6)$$

TABLE 1: Notations' variables used in this article.

Notations	Description	Units
O	Origin or centre of the roundabout	
α	Angle between two radian points	
α_x	Angle between two radian points of auxiliary queuing lane	
q_x	Limited vehicles queue before second stop-line from approach x	m
r	Radius of the roundabout	m
C_x^l	No. of possible vehicle's queue on the approach x	m
I_{avg}^x	Average occupied space of a single vehicle	m
C_n^x	Left-turning lanes in circulatory roadway for the approach x vehicles	m
n	No. of vehicles	
C_c^l	Capacity of circulatory roadway for left-turn vehicles	Pcu/h
W_w	Weaving width of circulatory roadways	m
e_1	Entry lane	
e_2	Exit lane	
S_{CL}	Signal cycle length	s
L	Total lost time	s
$\sum_{j=1}^k x$	Total no. of phases j to k for approach x	s
Y_j	Saturation flow towards circulatory roadway by using phase j	Pcu/h
l_j	Lost time during signal cycle	s
R	Total lost time of red light during change cycle	s
t_{cx}	Time to leave vehicle before second stop line (SL) from approach x	s
S_{cf}	Saturation flow of circulatory roadway	Pcu/h
G_{tc}	Effective green total time per cycle	s
G_x^0	Effective green time for approach 1	s
G_{x+1}^0	Effective green time for approach 2	s
G_{x+2}^0	Effective green time for approach 3	s
S_x	Saturation flow rate of straight-going traffic at approach x	Pcu/h
V_x	Traffic flow rate of approach x	Pcu/h
$t_{x+1,x+2}^a$	Green time adjustment of straight-go flow of approach (2, 3)	s
Y_x^s	Saturation flow rate of straight-go traffic of approach x	Pcu/h
w	Width of one circulatory lane of roundabout	m
G_x^s	Green time for straight-go traffic on approach x	s
q_x^l	Left-turn vehicle ratio from approach x	Pcu/h
y_x^f	Saturation flow rate for left-turn vehicles on approach x	Pcu/h
n_x^l	Limited no. of lanes for left-turn vehicles	
S_x^l	Saturation flow of left-turn lane on approach x	Pcu/h
G_x^l	Green time for left-turn flow before second stop line	s
I_x^d	Changing interval between G_x^d and G_x^s	s
$C_{OA d}$	Capacity of one approach direction	Pcu/h
C_R	Total capacity of TLSR-2SL	Pcu/h
C_{fs}^x	Capacity of first stop-line from approach x	Pcu/h
C_{ss}^x	Capacity of second SL from approach x	Pcu/h
n_{fs}^x	No. of straight-going lanes at first SL on approach x	
G_{fs}^x	Green time for first SL vehicles at approach x	s
C_{fs}^{xl}	Capacity of left-turn vehicles on approach x at first stop-line	Pcu/h
G_{fs}^{xl}	Green time of left-turn vehicles at first SL on approach x	s
n_{fs}^{xl}	No. of left-turn lanes at first SL on approach x	
q_x^c	Left-turn flow inside circulatory from approach x	Pcu/h

3. Mathematical Formulation of Optimal Signal Cycle and Capacity

Integration of optimal signal cycle length and capacity formulation is computed to evaluate the performance of the TLSR-2SL in this section.

3.1. Computation of Optimal Signal Cycle. Optimal signal cycle length (S_{CL}) is determined according to the Webster's equation rule, as shown in the following equation [28]:

$$S_{CL} = \frac{(1.6L + 5)}{\left(1 - \sum_{j=1}^k Y_j\right)}, \quad (7)$$

where 1.6 s is the start-up delay of a vehicle. The total lost time (L) can be computed, as follows:

$$L = \sum_{j=1}^k l_j + R. \quad (8)$$

For calculating total green time per cycle (G_{tc}), the following equation is computed and is given as follows:

$$G_{tc} = S_{CL} - L. \quad (9)$$

As presented in Figure 3, there are three possible approaches to the roundabout. Suppose approaches 1, 2, and 3 are called x , $x + 1$, and $x + 2$, respectively. Approaches 2 and 3 have opposite directions, and they both use the exact green phase timing for straight-go flow G_{x+1}^0 and G_{x+2}^0 , whereas approach 1 uses another phase timing, as given in the following equations:

$$G_{x+1}^0 = G_{x+2}^0 = G_{tc} \max\left(\frac{V_{x+1}}{S_{x+1}}\right), \quad (10)$$

$$G_{x+1}^0 = G_{x+2}^0 = G_{tc} \max\left(\frac{V_{x+1}/S_{x+1} + V_{x+2}/S_{x+2}}{\sum_{j=1}^k Y_j}\right), \quad (11)$$

where V_{x+1} , S_{x+1} and V_{x+2} , S_{x+2} are traffic and the saturation flow rate of straight-go traffic from approaches 2 and 3, respectively. Moreover, the following equation is formulated for approach 1 as follows:

$$G_x^0 = G_{tc} \max\left(\frac{V_s/S_x}{\sum_{j=1}^k Y_j}\right). \quad (12)$$

3.2. Green Time Adjustment for Straight-Go Traffic. The possible flow rates of $x + 1$ and $x + 2$ have behaved differently in some states; in addition, G_{x+1}^0 and G_{x+2}^0 might have different values and need to adjust for getting similar degrees of saturation flow. The adjustment of green time for straight-go traffic flow ($t_{x+1,x+2}^a$) is formulated in the following equations:

$$t_{x+1,x+2}^a = G_x^0 \left[1 - \frac{(\min(y_{x+1}^s), y_{x+2}^s)}{\max(y_{x+1}^s, y_{x+2}^s)} \right], \quad (13)$$

$$G_x^s = G_x^0 - \beta * t_{x+1,x+2}^a + \delta * t_x^a, \quad (14)$$

where t_x^a is used for green time adjustment for traffic flow coming from the south-to-west direction. Moreover Y_x^s , Y_{x+1}^s , and Y_{x+2}^s are used for a saturation flow rate of approach 1. The straight-go traffic of approaches 2 and 3, as well as β and δ conditions, are given in the following equations:

$$\beta = \begin{cases} 1, & Y_{x+1}^s < Y_{x+2}^s, \\ 0, & Y_{x+1}^s \geq Y_{x+2}^s, \end{cases} \quad (15)$$

$$\delta = \begin{cases} 1, & Y_x^s > 0, \\ 0, & Y_x^s \leq 0. \end{cases} \quad (16)$$

3.3. Green Time Adjustment for Left-Turn Flow at First Stop Line. The capacity of circulatory roadway for left-turning flow (C_c^l) is considered for determining the green-time of left-turn traffic besides the second stop line (G_x^l) as computed in the following equation:

$$G_x^l = \begin{cases} \min\left(G_x^s, \frac{C_c^l}{n_x^l S_x^l}\right), & q_x^l G_{tc} \geq C_c^l, \\ G_x^s, & q_x^l G_{tc} < C_c^l \text{ and } Y_x^l \geq Y_x^s, \\ G_x^s Y_x^l, & q_x^l G_{tc} < C_c^l, \text{ and } Y_x^l < Y_x^s. \end{cases} \quad (17)$$

3.4. Green Time Adjustment for Left-Turn Flow at First Stop Line. As shown in Figure 3, the left-turn flow from the east before the second stop line DD' has a conflict with the west vehicles, as shown in equation (17). Thus, the green time for straight-go traffic (G_x^s) should be equal to or greater than green-time for left-turning flow (G_x^l), which means that the green time for straight-go traffic is more than or equal to left-turning flow ($G_x^s \geq G_x^l$), as obtained in the following equation:

$$G_x^l = S_{CL} - 2I_x^d - G_{x+2}^s. \quad (18)$$

Based on these estimations, we propose a general signal timing model for TLSR-2SL. The proposed computation can be equally used for T-shape intersection by adjusting the signal timing parameters, as shown in Figure 1(c).

3.5. Capacity. For nonsignalized roundabouts, there are two methods to measure the capacity, namely, the gap acceptance theory and linear regression model as discussed in Highway Capacity Manuals (HCM) [29] and Roundabout: an information guide [30]. However, these models are not applicable for a signalized roundabout, and several studies have concluded and obtained a calculation-based formula according to a saturation flow rate formula (e.g., $3600/t_f$), vehicles/hour/lane, where t_f considers as a headway gap for straight-go and left-turning traffic. For example, in [7], scholars use 1650 pcu/h and 1550 pcu/h per lane for straight and left-turning traffic with a minimum headway [2.2~2.3 s]. Apparently, literature shows that measuring left-turning flow is crucial for the signalized intersection and roundabout to analyze full capacity. Due to less innovation on the impacts of a traffic signal in circulatory lanes, there are still numerous gaps in left-turning capacity analysis. This research also works along with the line of filling this research gap.

However, multiple capacities are computed to estimate TLSR-2SL performance analysis: capacity measurement of east left-turning vehicles via stopping at second stop line to exiting south, the flow from second signalized stop line to south section, and E-W (through lane) capacity. In addition, the equation of the overall capacity of one approach direction can be derived from the roundabout capacity (C_R) as given in the following equation:

$$C_R = \sum_{k=1}^x (C_{fs}^x + C_{ss}^x). \quad (19)$$

The capacity of one approach direction C_{OAd} (e.g., E-W) can be computed by using the following equation:

$$C_{OAd} = (C_{fs}^x + C_{fs}^{xl}), \quad (20)$$

where the capacity of through lane (C_{fs}^x) can be further calculated using

$$C_{fs}^x = n_{fs}^x S_x \left(\frac{G_{fs}^x}{S_{CL}} \right). \quad (21)$$

The capacity of the second stop line (C_{ss}^x) from approach x is computed by

$$C_{ss}^x = \min\{C_{fs}^{xl}, C_c^l\}. \quad (22)$$

The left-turning second stop-line capacity to the south (E-S) via second signalized stop line can be computed using

$$\sum\{C_{fs}^{xl}, C_{ss}^x\} = n_{fs}^{xl} S_x^l \left(\frac{G_{fs}^{xl}}{S_{CL}} \right). \quad (23)$$

Meanwhile, C_x^{w-a} is the capacity of the waiting area, as shown in Figure 1(d), and computed according to

$$C_x^{w-a} = \bar{V}_{avg} + sd, \quad (24)$$

where \bar{V}_{avg} is an average length of the vehicle and sd is the safe distance between the first vehicle of stop line and the last vehicle about to waiting area. To accommodate one heavy vehicle, \bar{V}_{avg} is considered as 17 m and sd as 3 m; C_x^{w-a} should not be less than 20 m.

4. Numerical Analysis

4.1. Description of Simulator and Model Calibration. To execute TLSR-2SL, authors took an upgraded isolated prototype to investigate both spatial and temporal constraints that affect the capacity most, as depicted in Figure 2. Then, the prototype structure is appropriately drawn in an Aimsun Next microscopic simulator to conduct the sensitivity tests, using a two-lane-car-following model. According to the minimum conflict point, the roundabout priority rules are settled using a default setting. Thus, the accumulative flow analysis of every arm (straight and left-turning) ratio is concluded separately to evaluate the TLSR-2SL performance. Moreover, the straight and left-turning flow is assumed as 1650 Pcu/h and 1550 Pcu/h according to HCM recommended guidelines with a minimum headway of [2.2 s~2.3 s] [31].

Based on presumption, the vehicle tends to avoid shallow cruising speed or more than 50 km/h velocity, while crossing the circulatory roadway. According to the Chinese and European DOT conventions, the traffic on the roads keeps on the left hand, and the vehicle flow pattern relies on roundabout geometric structure [5]. Moreover, each method is executed three times in series to obtain simulation outputs and minimize the expected errors. In addition, the right-turning flow of each approach is not controlled by signals; in addition, pedestrians and nonmotor vehicles are assumed to cross during the red phase time.

4.2. TLSR-2SL Performance Analysis. This section investigated the precision analysis of the proposed TLSR-2SL in terms of left-turning capacity and their relative error ratios and compares them with the simulator benchmark values as well as the other model without supposing the internal space constraints. The model without considering the internal space area has one signalized stop line at the roundabout entrance, as shown in Figure 1(b). Meanwhile, Aimsun Next microscopic simulator is employed for simulations to obtain the capacity values of the proposed and other models under multiple signal cycles and roundabout radius, as presented in Figures 5(a) and 5(b) [21, 32, 33].

Hereafter, the models' performance is based on the given three aspects: (1) changing the optimal signal cycling length of the roundabout, where the minimum and maximum signal cycle length are set from [60 s~160 s] and the central radius from [10 m~60 m], as presented in Figure 5(b). Moreover, the duration of signal cycle length is T/3 equally for each phase with starting loss time of vehicle 2 s. One possible reason is that fewer phases acquire less clearance time and improve transportation efficiency. In Step (2), after compilation of signal cycles, each model's average left-turning flow/lanes capacity is obtained from the simulator. Also, the entry volume is used equally for all models because the changes in datasets (entry volume) significantly impact the model's operational performances during the executed simulations.

Finally, in Step (3), comparative performance analysis of left-turning flow between aforesaid models is presented in Table 2. It is easy to comprehend that the proposed TLSR-2SL has greatly improved the capacity when the internal space constraints are considered. On the other hand, the capacity throughput of the traditional model without supposing internal space area has a more significant relative error than Aimsun benchmark values, and the average error is above 20%. However, the improved capacity using the TLSR-2SL is approximately 15.1% compared with base values. One of the possible reasons is that if traffic signals employ just at entry lanes without considering a second signalized stop line, then the roundabout is equivalent to a large-size intersection, which not only requires a longer inter-green time for a single approach to clear but also to lose the effective-green time in one signal cycle. During the high flow, the circulatory weaving points of the model without considering internal constraints is severe and retards operational performance. The summary of analysis shows that the relative error of the proposed model compared to benchmark values is within 10%, where the maximum and minimum relative error ratios are 13.1% and 1.02%.

4.3. Sensitivity Tests. To investigate the TLSR-2SL deeply, sensitivity analysis is then elaborated to examine how spatial and temporal parameters affect the capacity of the signalized roundabout, as presented in Figure 6. As shown in Figure 6(a), the capacity of straight-traveling stream is directly proportional to signal cycle lengths and the inscribed radius of the roundabout, as the central radius (R) increases than the through lane flow. One of the possible reasons is

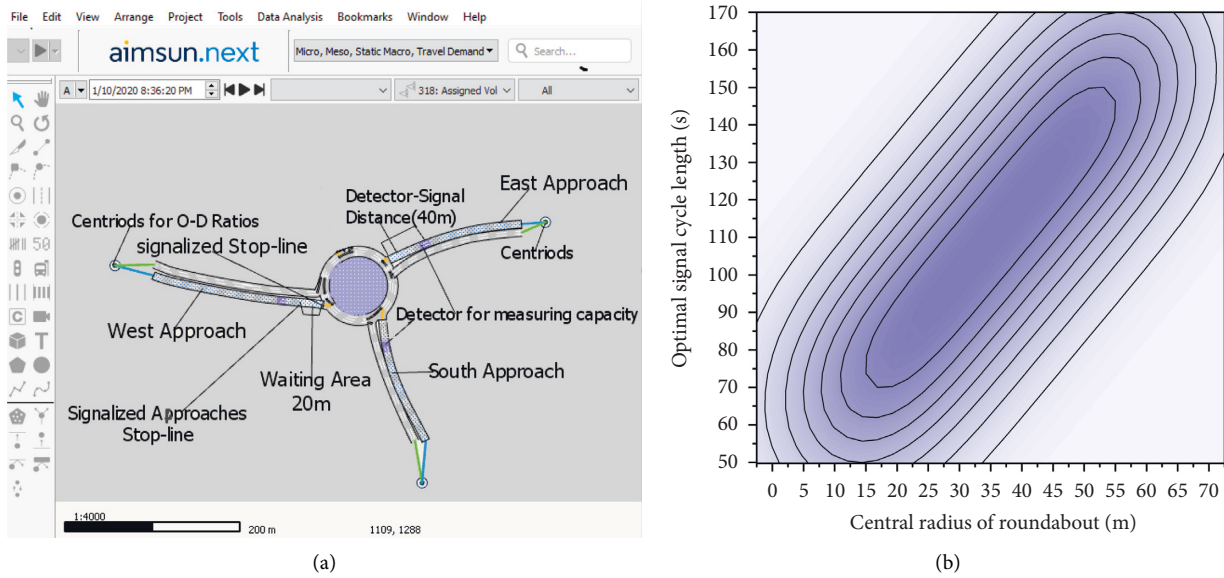


FIGURE 5: Optimal signal cycle length with respect to inscribed island radius and Aimsun simulator. (a) Aimsun Next simulator. (b) Optimal signal cycles' lengths.

TABLE 2: Left-turn capacity analysis of the proposed model.

Signal cycle length	Aimsun simulator benchmark values (Pcu/h)	Model without considering internal space area		Proposed TLSR-2SL model considering internal space area		Improved ratio of accuracy level by using TLSR-2SL (%)
		Results (Pcu/h)	Relative error (%)	Results (Pcu/h)	Relative error (%)	
60	293	304	3.8	305	4.1	-0.4
75	413	318	-23.0	375	-9.2	13.9
90	406	329	-19.0	459	13.1	5.9
105	489	337	-31.1	494	1.02	30.1
120	523	346	-33.8	538	2.9	30.9
135	474	349	-26.4	496	4.6	21.9
150	397	351	-11.6	425	7.05	4.6
160	426	354	-16.9	404	-5.16	11.7

that longer signal cycle lengths direct to fewer switching of phase interval, as defined by the Webster equation method. Hereafter, when the roundabout radius is larger, the approaching velocity of passing vehicles inside the circulatory roadways is likewise higher. Therefore, more prominent roundabouts/intersections require a larger signal cycle to facilitate more vehicles in specific threshold time.

Figure 6(b) presents a microscopic view of left-turning flow, elaborating the impacts of the signal cycle with respect to central island radius. Left-turning flow is entirely dependent and relies on the central island and approaching left-turning lanes, as the volume of the rotary increases, then the flow also upsurges. In the proposed lane-marking scenario, the signal cycle length has a complicated relationship with left-turning traffic, at the initial stages of $R = 30$ m, the capacity escalates with the step-up of the signal cycle, and then slightly depreciates after reaching a specific threshold level. For instance, the shorter radius with lower signal cycle spill-back the left-turning flow. One specific reason for this revert-back situation, some straight-going vehicles may use

left-turning lanes or vice versa. The second possibility is a shorter signal cycle or radius, which does not have enough storage space to facilitate excessive queuing of vehicles. Moreover, in light of a longer signal cycle (100 s~120 s) with ($R = 30$ m~40 m) central radius, first gain the capacity level as the signal cycle increase, and after touching extreme values, the capacity decreases as the cycle length increases. In contrast, above 40 m radius, the flow is almost linear without any deadlock conditions, showing that the proposed recoating model performs better in higher signal cycles and radius than shorter ones. The computation reasoning of this phenomenon is further elaborated in the below discussion in Section 5. Nonetheless, in the radius ranges from ($R = 50$ m~60 m), the maximum capacity is almost moderate as 500 Pcu/h.

To achieve a state-of-the-art temporal threshold, the optimal signal timing should not be exceeded or less to fulfill the first queuing area at signalized curvature or second signalized spiral-mark storage space. In the first case, if the signal timings threshold is less for left-turning flow, then

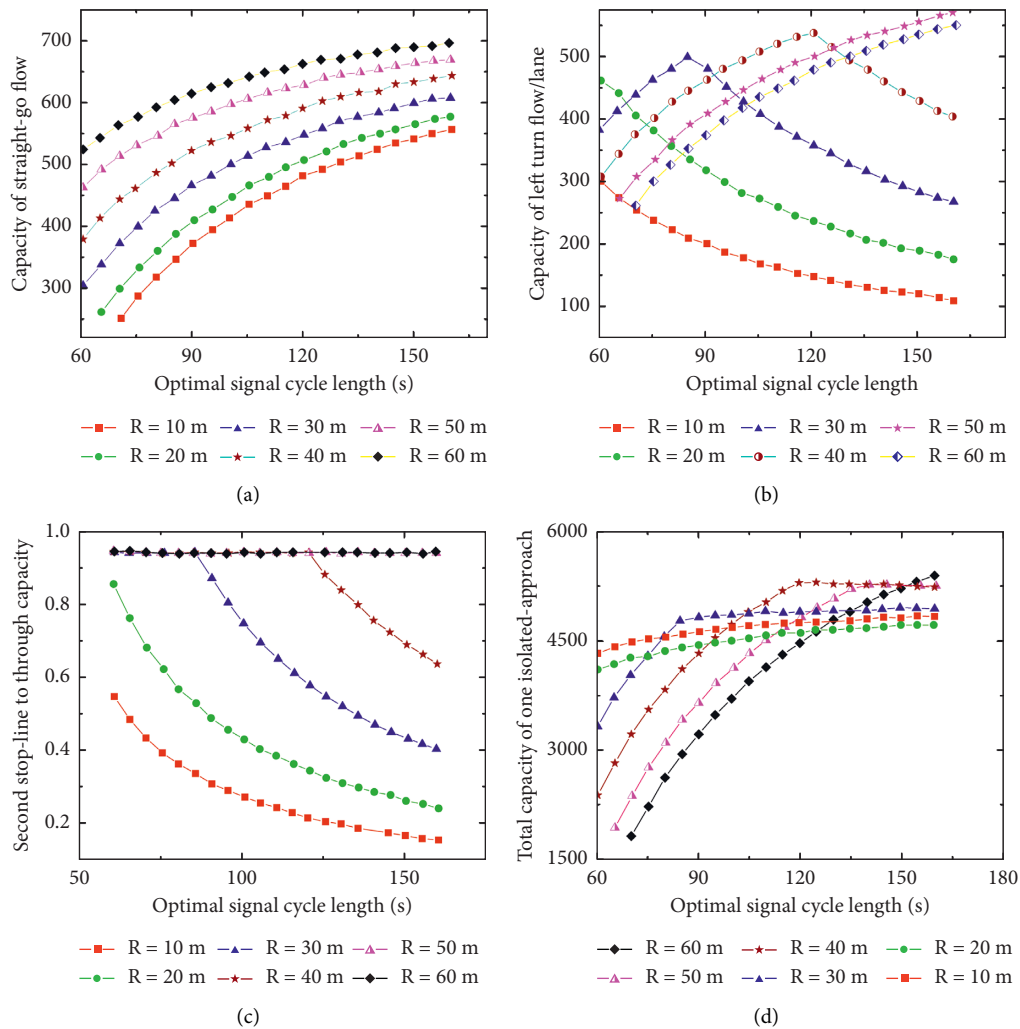


FIGURE 6: Model sensitivity analysis under different signal cycles and radius. (a) Capacity of straight-go flow. (b) Capacity of left-turning flow/lanes. (c) Second stop-line to straight-go flow. (d) Overall capacity of one approach direction.

internal space constraints cannot fully engage the queuing space to utilize the available gaps. On the other hand, in the second scenario, if the signal timings are larger, then, due to specific limits of vehicles arrivals, a deadlock situation can occur inside the circulatory stream and weaving points, induces higher delay, and retards the operational fluency.

Mainly, determining an optimal signal cycle is considered one of the essential fundamental parameters during the computations of signal timings. It is famous for the classic timing theory that longer signal cycles acquire longer clearance time to facilitate a higher flow level. Optimal cycling is based on minimum overall delay time, especially at a signalized intersection. As shown in Figure 6(b), smaller signal cycles having a smaller central radius of the roundabout are affected and spill-back their capacity or face a locking up situation. To resolve such small errors up to some extent for isolated-roundabouts, optimal signal cycling can also be achieved under the objective of capacity maximization.

Figure 6(c) illustrates the possible E-S (second stop line to south direction) flow ratios variations. Nevertheless, in

Figure 6(d), it is obvious that when the signal cycle is lower with a lower central radius, the total capacity of one approach direction is also sensitive to analysis. However, under the higher signal cycle length and radius, the capacity of one approach direction is almost linear.

4.4. Left-Turning Capacity under Proportion of Heavy Vehicles. The challenges faced by heavy vehicles at roundabouts associated with adverse drivers experiences inevitably result in lower capacity and follows perennial congestion. The author's performed a capacity analysis of left-turning flow to check the applicability of the proposed model under the 5% proportion of heavy vehicles. The comparative throughput between TLSR-2SL, T-intersection, and model without considering internal space constraints are evaluated under [60 s~160 s] signals cycles with [10 m~60 m] radius of the roundabout, as illustrated in Figure 7 [21].

As depicted in Figures 7(a) and 7(b), under the [60 s~80 s] signal cycle with a 5% proportion of heavy vehicles is taken into consideration, whereas the left-turning

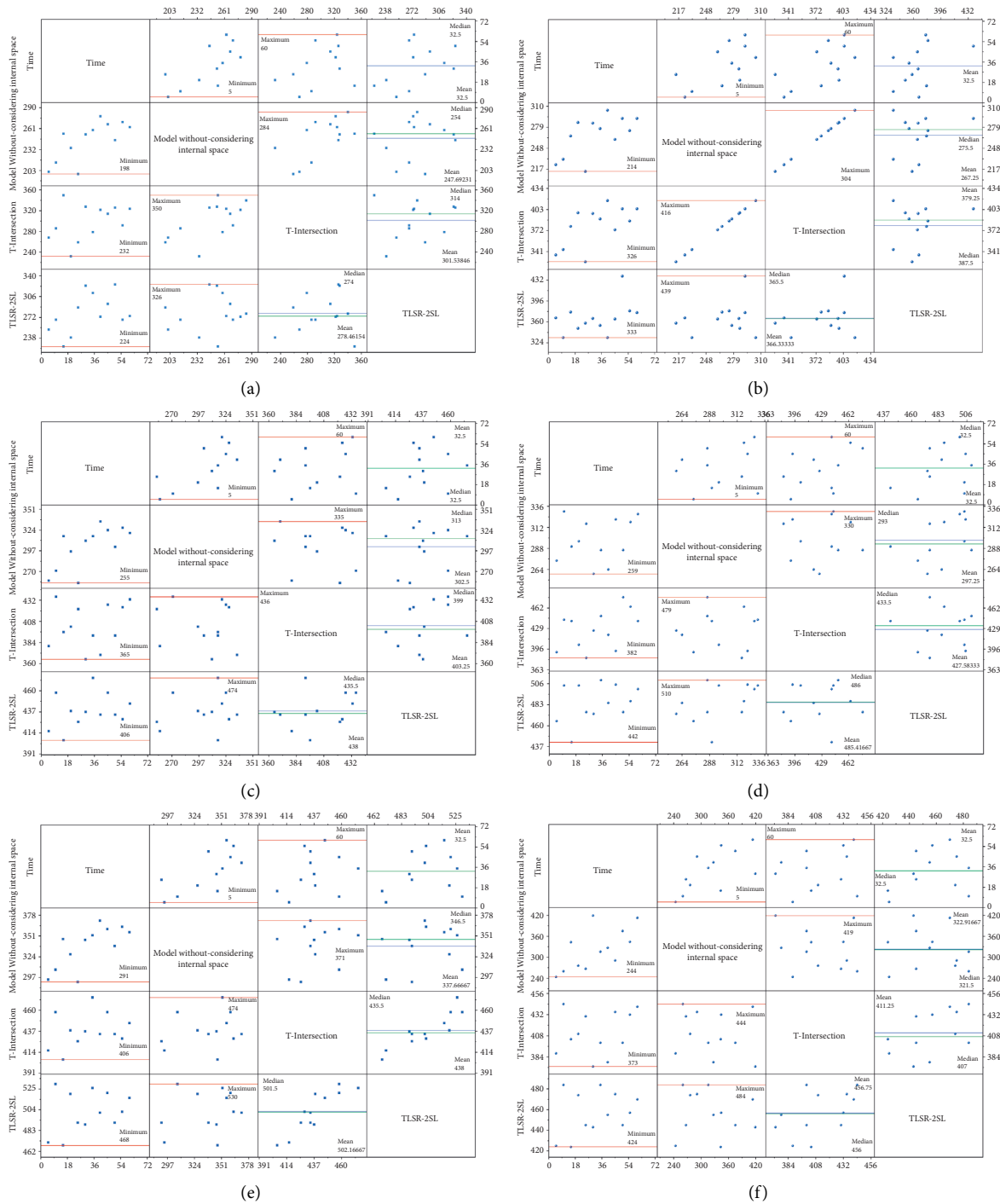


FIGURE 7: E-S flow under [60 s~160 s] signal cycle with 5% proportion of heavy vehicles. (a) 60s signal cycle with 10 m radius. (b) 80 s signal cycle with 20 m radius. (c) 100 s signal cycle with 30 m radius (d) 120 s signal cycle with 40 m radius. (e) 140 s signal cycle with 50 m radius. (f) 160 s signal cycle with 60 m radius.

flow under the T-shape intersection outperforms TLSR-2SL, and the proposed model performs better than the model without considering internal space constraints. A shorter signal cycle with an increment of heavy vehicles and the steady turbulence in left-turning flow is considered possible reasons, about to repress the functional fluency of TLSR-2SL. Besides that, the flow under [100 s~120 s] signal cycle with a radius of [30~40 m] of the proposed method

performed better than T-intersection and another model. However, the average flow differences between T-intersection and TLSR-2SL models are approximately [403~427 pcu/h] and [438~485 pcu/h], as illustrated in Figures 7(c) and 7(d). It is noteworthy to mention that left-turn short lane accommodates more left-turning flow than the intersection, if the radius should be more than 20 m, as proved in below discussion section.

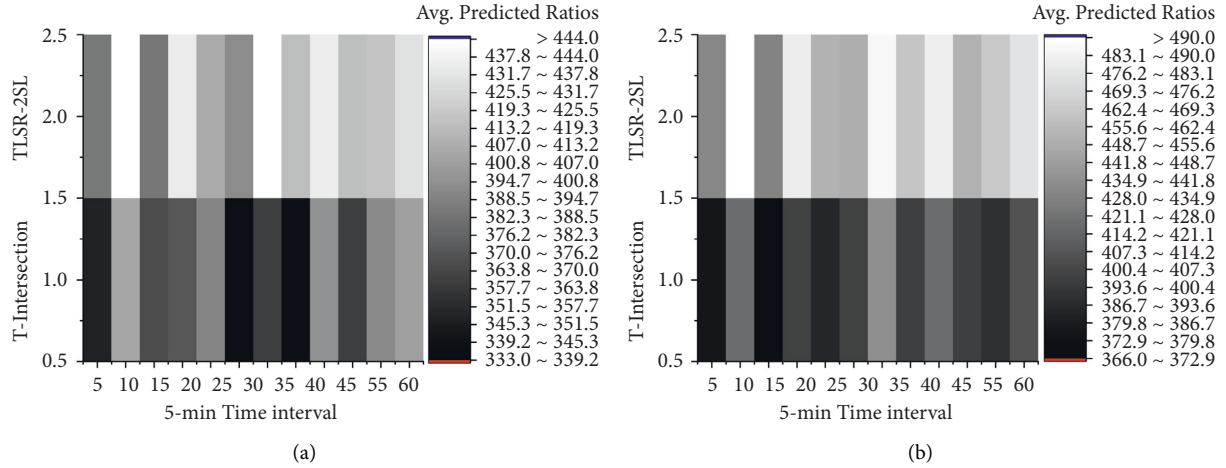


FIGURE 8: E-S flow comparative analysis between T-intersection and TLSR-2SL. (a) 140 s signal cycle with 50 m radius. (b) 140 s signal cycle with 60 m radius.

This phenomena is further elaborated to investigate signal cycle [140 s~160 s] with [50 m~60 m] radius, as shown in Figures 7(e) and 7(f). The executed simulations show that the proposed model is a promising way to improve the left-turning stream including heavy vehicles. In addition, TLSR-2SL is performing better than other approaches, and other methods are suitable if the passing left-turning flow should be between 300 and 350 Pcu/h to accommodate in nonpeak hours, effortlessly. It was also observed that the flow becomes more efficient if the signal cycle length increases from 100 s to [140 s~160 s] for [50 m~60 m] radius.

During the simulation execution process, the flow under intersection and model without considering internal space constraints seem to idle at the beginning of green time and improves flow as the green time near to terminate, which considers the poor impacts for signalized junctions. Meanwhile, the capacity of the TLSR-2SL model has to maintain its consistency and reliability and presents expected results during the simulations process.

Apparently, the appropriate length of phase-timing and radius are the main factors that gain the flux uniformly of the proposed approach compared with other techniques. It is noteworthy mentioning that if the proportion of heavy vehicles increases, a higher signal cycle likewise improves and facilitates more vehicles and improves safety. On the other hand, models under [140 s~160 s] signal cycle have improved [12%~14%] left-turning flow compared to T-intersection.

In the aforementioned perspective of the proposed TLSR-2SL, authors also examined [140 s~160 s] signal cycles with radius [50 m~60 m] under bad weather conditions. The applicability and impact under different resisting weather scenarios (e.g., windy, rainy, or snowy, etc.) for left-turning flow also give auspicious outputs, as presented in Figures 8(a) and 8(b), where the proposed model is performing better than a signalized intersection. Yet, the comparative study between a signalized roundabout and intersection has not received deep intentions. However, these comparisons are justifiable because of using the same Webster equation method to evaluate the signal timings for each intersection/roundabout equally.

5. Discussions

If the circulatory roadway is small and has a limited number of vehicle queues (C_n^x) before the second signalized stop line, then this traffic-control method may not be used. As shown in equations (2) and (3), C_n^x is entirely reliant on the central island r ; also the number of left-turning lanes is dependent on the circulatory roadway n . However, the following equation should be satisfied to pass all left-turning vehicles in one signal cycle:

$$C_n^x \geq S_{CL} q_x^l \quad (25)$$

From equations (2)–(4), we have

$$C_n^x = \frac{n\pi\alpha_x}{180l_{avg}(r + 0.5w)} \quad (26)$$

Then, from the above equations, we get

$$r \geq \frac{180q_x^l S_{CL} l_{avg}}{n\pi\alpha_x - 0.5w} \quad (27)$$

Let there be two left-turning E-S lanes on the circulatory roadway, $\alpha_x = 120$, $S_{CL} = 130$ s, $l_{avg} = 4.5 \sim 5$ m, and $w = 3.7$ m; therefore, r should not be less than 20 m to satisfy left-turn traffic almost of $q_x^l = 500$ Pcu/h from one approach.

Compared with the previous method of signal-control, the control method in this paper eliminates all conflict points at weaving sections of the roundabout with the at-least two circulatory lanes.

6. Concluding Remarks

Implementation of optimal signalization with the modern lane markings is considered an effective way to enhance the operational performance of roundabouts. To control the left-turning flow movement, this research presented the TLSR-2SL framework based on two signalized stop lines. The second stop line is exclusively set in the circulatory roadway with an additional lane model. The optimal signal cycles and capacities equations are derived

to evaluate the impacts of the proposed approach. Multiple sensitivity tests revealed that the output of executed simulations helped to avoid spatial and temporal gaps in the circulatory lanes and decreased the conflicts at weaving points excessively. Also, the engineering-oriented approach appears to reinforce a clear set of priorities to improve the roundabout flow, especially to assist left-turning flow that regulate circulating traffic streams efficiently and strengthen the lane-guidance for drivers by offer exiting priorities.

However, there was less work to define the comparative study of left-turning capacity differences for the T-shape roundabout, as presented in this article. The conducted study conclusively showed the following: (1) the sensitivity analysis of the proposed method outperformed benchmark methods; (2) TLSR-2SL was performing better than T-intersection and traditional model under [100 s–160 s] signal cycles with radius [30 m~60 m] and well cooperative to improve the promising left-turning flow; (3) the model performance shows that the left-turning flow capacity could be improved 15.1%, and controlled relative error within 10%; (4) single approach flow can also improve by using the method in moderate demand; (5) based on assumptions, the overall roundabout capacity increased, and travel delay decreased efficiently; (6) hence, under proposed paradigm, the speed trajectory near to roundabout relatively performed better than other methods. Consistent with these findings, the number of observed potential conflicts was marginally reduced, and the proposed method was helpful to improve mobility with its distinctly different concept in peak hours. Alternatively, traditional marking systems affected driver behavior, level-of-service, and safety performance. However, the framework in minor traffic flow had no significant impacts.

In future research directions, special lanes and defined pathways for pedestrian and nonmotor vehicles are also taken into consideration along with the proposed model. It is a challenging issue in intelligent transportation systems, especially in commercial districts during rush hours. However, many economies have taken serious steps to address this content resulting in an ongoing repainting of signalized roundabouts to decrease the number of accidents and average delay time. In addition, proper calibration of roundabout fundamental parameters is essential to reduce green-loss time and improve saturation flow, particularly the roundabout having lanes of the individual-arm more than two or giant inscribed radius.

Data Availability

Some or all data, models, or code that support the findings of this study are available from the corresponding author upon reasonable request.

Conflicts of Interest

The authors declare no potential conflicts of interest with respect to the research, authorship, and/or publication of this article.

Acknowledgments

The authors acknowledge the support from China Scholarship Council.

References

- [1] Z.-H. Jiang, T. Wang, C.-Y. Li, F. Pan, and X.-G. Yang, "Investigation on two-stop-line signalized roundabout: capacity and optimal cycle length," *Journal of Advanced Transportation*, vol. 2019, Article ID 5720290, 9 pages, 2019.
- [2] X. Yang, X. Li, and K. Xue, "A new traffic-signal control for modern roundabouts: method and application," *IEEE Transactions on Intelligent Transportation Systems*, vol. 5, no. 4, pp. 282–287, 2004.
- [3] T. Tollazzi, R. Mauro, D. Žilionienė, I. I. Otković, and N. Stamatidis, "Modern roundabouts: a challenge of the future," *Journal of Advanced Transportation*, vol. 2019, Article ID 3950891, 2 pages, 2019.
- [4] J. Zhao, K. K. Kigen, and M. Wang, "Modelling the operation of vehicles at signalised intersections with special width approach lane based on field data," *IET Intelligent Transport Systems*, vol. 14, no. 12, pp. 1565–1572, 2020.
- [5] W. D. Division, *Roudabouts, M22.01, WSDOT Design Manual*, Chapter 1320, Transportation Research Board, National Research Council, pp. 1–26, Washington, DC, USA, 2020.
- [6] K. Toddr, "A history of roundabouts in Britain," *Transportation Quarterly*, vol. 45, pp. 143–155, 2006.
- [7] B. N. Persaud, R. A. Retting, P. E. Garder, and D. Lord, "Safety effect of roundabout conversions in the United States: empirical Bayes observational before-after study," *Transportation Research Record: Journal of the Transportation Research Board*, vol. 1751, no. 1, pp. 1–8, 2001.
- [8] Y. Bie, S. Cheng, S. M. Easa, and X. Qu, "stop-line setback at a signalized roundabout: a novel concept for traffic operations," *Journal of Transportation Engineering*, vol. 142, no. 3, Article ID 05016001, 2016.
- [9] C. J. Lines, "Cycle accidents at signalized roundabouts," *Traffic Engineering and Control*, vol. 36, no. 2, pp. 74–77, 1995.
- [10] Aashto, "The Highway Safety Manual, American Association of State Highway Transportation Professionals," Washington, D.C, WA, USA, 2010, <http://www.highwaysafetymanual.org>.
- [11] I. Anderson and K. W. Martin, "Traffic flow improvements at newbridge roundabout," *Seventh International Conference on Road Traffic Monitoring and Control*, vol. 391, no. 391, pp. 101–105, 1994.
- [12] E. A. A. Shawaly, C. W. W. Li, and R. Ashworth, "Effects of entry signals on the capacity of roundabout entries. A case-study of Moore Street roundabout in Sheffield," *Traffic Engineering and Control*, vol. 32, no. 6, pp. 297–301, 1991.
- [13] S. C. Wong, N. N. Sze, B. P. Y. Loo, A. S. Y. Chow, H. K. Lo, and W. T. Hung, "Performance evaluations of the spiral-marking roundabouts in Hong Kong," *Journal of Transportation Engineering*, vol. 138, no. 11, pp. 1377–1387, 2012.
- [14] Q. Liu, X. Zhou, and J. Zhao, "Modeling the operation of left-turn vehicles at exit lanes for left-turn intersections," *Journal of Transportation Engineering, Part A: Systems*, vol. 147, no. 5, Article ID 04021022, 2021.
- [15] K. Xue, X. Yang, and Y. Bai, "Optimization of control method for roundabout at fixed cycle," *Journal of Highway and Transportation Research and Development*, vol. 21, no. 5, pp. 83–87, 2004.
- [16] I. M. Abuamer and H. B. Celikoglu, "Local ramp metering strategy ALINEA: microscopic simulation based evaluation

- study on istanbul freeways,” *Transportation Research Procedia*, vol. 22, pp. 598–606, 2017.
- [17] R. Akçelik, “Roundabout metering signals: capacity, performance and timing,” *Procedia-Social and Behavioral Sciences*, vol. 16, pp. 686–696, 2011.
- [18] W. Ma, Y. Liu, L. Head, and X. Yang, “Integrated optimization of lane markings and timings for signalized roundabouts,” *Transportation Research Part C: Emerging Technologies*, vol. 36, pp. 307–323, 2013.
- [19] X. Yang, X. Li, G. Zhou, Y. Lin, J. Yang, and K. Xue, “The traffic control and management system for large roundabout,” in *Proceedings of the 8th World Congress on Intelligent Transportation System*, Sydney, Australia, October, 2001.
- [20] A. S. M. Bakibillah, M. A. S. Kamal, C. P. Tan, S. Susilawati, T. Hayakawa, and J.-I. Imura, “Bi-level coordinated merging of connected and automated vehicles at roundabouts,” *Sensors*, vol. 21, no. 19, p. 6533, 2021.
- [21] P. Çalışkanelli, M. Özuysal, S. Tanyel, and N. Yayla, “Comparison of different capacity models for traffic circles,” *Transport*, vol. 24, no. 4, pp. 257–264, 2009.
- [22] R. Guo, L. Liu, and W. Wang, “Review of roundabout capacity based on gap acceptance,” *Journal of Advanced Transportation*, vol. 201911 pages, Article ID 4971479, 2019.
- [23] B. Al-Omari, H. Al-Masaeid, Y. Al-Shawabkah, Development of a delay model for roundabouts in Jordan,” *Journal of Transportation Engineering*, vol. 130, no. 1, pp. 76–82, 2003.
- [24] H. M. Al-Madani, “Dynamic vehicular delay comparison between a police-controlled roundabout and a traffic signal,” *Transportation Research Part A: Policy and Practice*, vol. 37, no. 8, pp. 681–688, 2003.
- [25] F. F. Saccomanno, F. Cunto, G. Guido, and A. Vitale, “Comparing safety at signalized intersections and roundabouts using simulated rear-end conflicts,” *Transportation Research Record: Journal of the Transportation Research Board*, vol. 2078, no. 1, pp. 90–95, 2008.
- [26] A. K. Patnaik, L. A. Agarwal, M. Panda, and P. K. Bhuyan, “Entry capacity modelling of signalized roundabouts under heterogeneous traffic conditions,” *Transportation Letters*, vol. 12, no. 2, pp. 100–112, 2018.
- [27] X. Sun, W. Ma, and W. Huang, “Comparative study on the capacity of a signalised roundabout,” *IET Intelligent Transport Systems*, vol. 10, no. 3, pp. 175–185, 2016.
- [28] N. J. Garber and L. A. Hoel, *Traffic & Highway Engineering*, PWS Publishing Company, Boston, MA, USA, 4th edition, 1983.
- [29] Transportation Research Board, *Highway Capacity Manual 2010 (HCM2010)*, Transportation Research Board, National Research Council, Washington, DC, USA, 2010.
- [30] Transportation Research Board and D. Washington, “National Cooperative Highway Research Program (Nchrp) Report 672,” *roundabouts: An Informational Guide*, Transportation Research Board, Washington, DC, USA, 2010.
- [31] P. Silburn, *Traffic simulation: Case for guidelines. EUR 26534*, Publications Office of the European Union; JRC88526, Luxembourg, Europe, 2014.
- [32] O. Hagrings, N. M. Roupail, and H. A. Sørensen, “Comparison of capacity models for two-lane roundabouts,” *Transportation Research Record: Journal of the Transportation Research Board*, vol. 1852, no. 1, pp. 114–123, 2003.
- [33] Z. Z. Tian and N. Wu, “Probabilistic model for signalized intersection capacity with a short right-turn lane,” *Journal of Transportation Engineering*, vol. 132, no. 3, pp. 205–212, 2006.